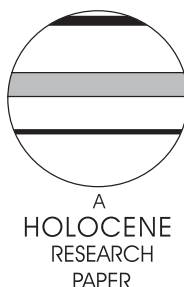


# Changes in late-Neoglacial climate inferred from former equilibrium-line altitudes in the Queen Elizabeth Islands, Arctic Canada

Gabriel J. Wolken,\* Martin J. Sharp and John H. England

(Department of Earth and Atmospheric Sciences, University of Alberta, Alberta T6G 2E3, Canada)

Received 8 February 2007; revised manuscript accepted 3 December 2007



**Abstract:** Regional-scale spatial variation in the change in equilibrium-line altitude (ELA) trend surface in the Queen Elizabeth Islands (QEI), Arctic Canada between the ‘Little Ice Age’ (LIA) and 1960 corresponds to Empirical Orthogonal Functions (EOFs) representing specific patterns of summer climate variability found in the modern record. Extreme warm (1953–1962) and cold (1965–1974) decades in the modern record were used as modern analogues of climatic conditions during the early twentieth century and the LIA, respectively. Because of the minimal influence of precipitation during both extreme decades, temperature is the variable upon which the fluctuation of the ELA is dependent. Hence, the ELA  $\Delta h$  pattern describes the spatial pattern of change in SAT across the QEI between the LIA and 1960. This pattern is consistent with the primary mode of variability of mean summer surface air temperature (SAT) in the modern record (ie, EOF-1, 1949–2002), the positive (negative) phase of which is strongly in place during the extreme warm (cold) decade. SAT anomalies in the QEI during the warm (cold) decade are positively correlated with a weak (strong) QEI-distal (QEI-proximal) polar vortex, higher (lower) than normal SSTs in the North Atlantic, and one of the lowest (highest) periods of sea-ice extent during the twentieth century. The climatic conditions during the cold decade are believed to describe conditions, which if sustained, would lead to a LIA-type cold episode capable of long-term snowline lowering and perennial snow/ice expansion. The climatic conditions during the warm decade represent possible modern analogues for those that might have occurred during the early twentieth century in the Canadian High Arctic, which led to a substantial reduction in perennial snow/ice.

**Key words:** Trimlines, ‘Little Ice Age’, snow extent, ice-cover change, glaciers, equilibrium-line altitude, climate variability, polar vortex, Arctic Canada, Queen Elizabeth Islands.

## Introduction

Climate change and the role of anthropogenic forcing have become focal issues in the last few decades, and concerns have escalated with regard to observed and predicted modifications to Polar Regions (Arctic Climate Impacts Assessment (ACIA), 2004). The most recognized impacts pertain to Northern Hemisphere sea ice reduction and thinning (Johannessen *et al.*, 1999; Vinikov *et al.*, 1999) and the simultaneous reduction of glaciers and ice caps that are contributing to global sea-level rise (Dyurgerov and Meier, 1997; Intergovernmental Panel on Climate Change (IPCC), 2001). Part of the problem with accurately assessing modern climate change is the inability to differentiate between changes resulting from natural climatic variability from those occasioned by forcing from greenhouse gases and sulphate

aerosols. This uncertainty is accentuated in the Canadian High Arctic because of the brevity of the instrumental record (~56 yr), which precludes direct observations of climate change prior to the mid-twentieth century. Consequently, one must rely on palaeoclimate proxies in high latitudes in order to better evaluate the record of natural variability; such records can be used as a baseline to better profile modern changes.

This study uses the change in the extent of perennial snow/ice and the variation in the equilibrium-line altitude (ELA) trend surface between the ‘Little Ice Age’ (LIA; ~AD 1250–1900, Grove, 2001) and 1960 in the Queen Elizabeth Islands (QEI; Figure 1). This comparison of LIA and 1960 ELAs records the impact of early twentieth-century warming in the Canadian High Arctic (Wolken *et al.*, 2008, this issue) and provides the basis for exploring the complex feedbacks internal to the climate system that may have contributed to these reported changes. The assumption is made that all atmosphere/ocean boundary conditions occurring

\*Author for correspondence (e-mail: gwolken@ualberta.ca)

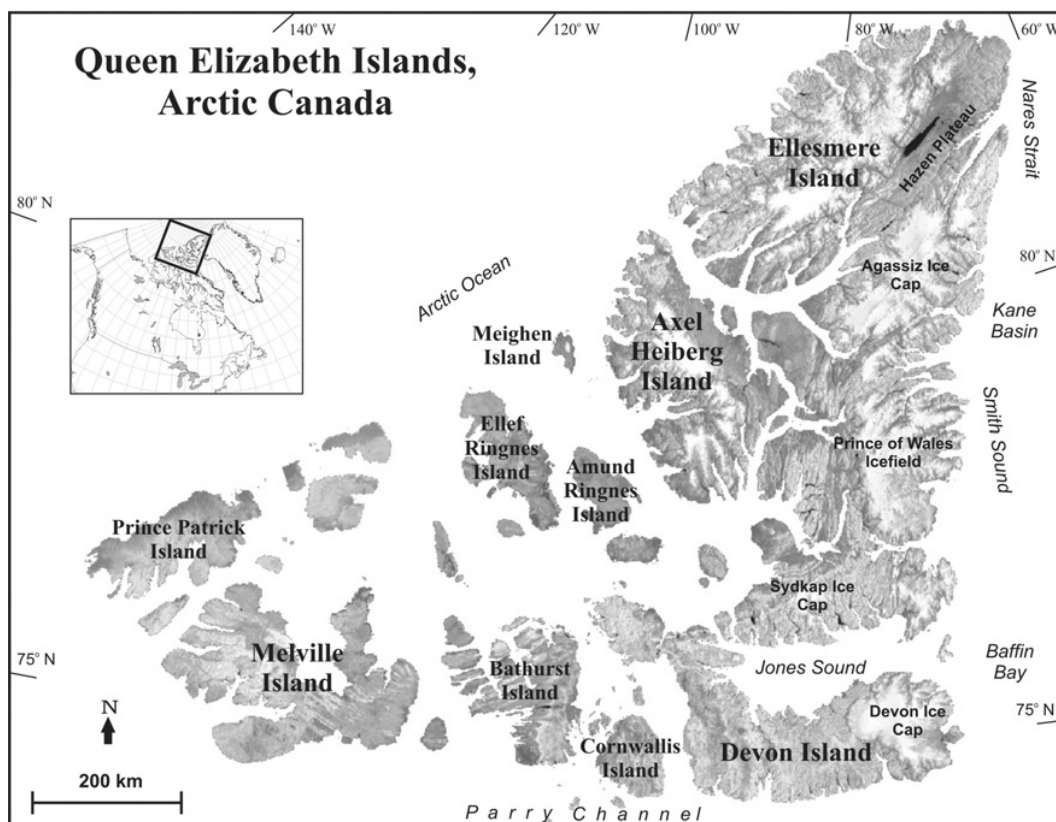


**Figure 1** Map of the Queen Elizabeth Islands, Arctic Canada (Radarsat Orthomosaic, courtesy of the Canadian Centre for Remote Sensing)

during the LIA and early twentieth century can also occur in the modern record. Thus, patterns of ELA  $\Delta h$  (the trend surface of difference in ELA; Wolken *et al.*, 2008, this issue) are referenced against specific modes of variability associated with climatological variables in the modern record (1949–2002) that serve as analogues for those that might have occurred during the early twentieth century in the Canadian High Arctic. Changes in the ELA ( $\Delta h$ ) from LIA to 1960 provide first-order estimates of climate change in the QEI and implicate possible patterns of atmospheric circulation that may explain the observed changes in early twentieth-century perennial snow/ice extent. The objective of the climatic analyses is to provide a better understanding of the synoptic scale conditions that influence the extent of terrestrial ice cover in Arctic Canada.

## Study area climatology

The climate of the Canadian Arctic is strongly influenced by complex interactions between the atmosphere, ocean, sea ice and land (Serreze and Barry, 2005). Although topographically diverse, most of the land surface of the QEI has been classified as polar desert, which is indicative of the aridity of this region. However, Maxwell (1981) partitions the Canadian High Arctic into climatic subregions, indicating high precipitation and greater warmth around Baffin Bay compared with colder areas in the more continental central and northwest QEI (Edlund and Alt, 1989). Systematic meteorological observations in the QEI began in the late 1940s, with the establishment of five coastal weather stations (Alert, Eureka, Mould Bay, Isachsen and Resolute Bay). Observations have been at times intermittent, and Mould Bay and

Isachsen have been closed in recent years. Efforts have been made to characterize the synoptic climatology of the region (Bradley, 1973, 1975; Bradley and England, 1978b, 1979; Alt, 1987), which revealed substantial variability in synoptic types and their influence on regional glaciers and ice caps.

## Data sources

### NCEP/NCAR reanalysis

The NCEP/NCAR reanalysis (NNR, following Bromwich *et al.*, 2002) uses data from 1948 to the present for data assimilation conducted four times per day (every six hours starting at 0Z), with a T-62 coordinate system (horizontal resolution of ~208 km) at 28 levels vertically (Kalnay *et al.*, 1996; Kistler *et al.*, 2001). As per standard procedure, these four times daily values are averaged, and the daily means are compiled to monthly means, which are then output to a global grid with a spatial resolution of  $2.5^\circ$  latitude by  $2.5^\circ$  longitude. The monthly mean data (1949–2002) for this study were obtained from the NCEP/ NCAR Reanalysis Project (<http://www.cdc.noaa.gov/cdc/reanalysis/reanalysis.shtml>) and include: 2 m temperature (hereafter referred to as surface air temperature, SAT); surface precipitation rate (SPR); sea-level pressure (SLP); and 850, 500 and 200 hPa geopotential heights. Gridded NNR variables are ranked according to the relative influence of observational data versus model output, where a rank of *A* indicates that the variable selected is most reliable, based strongly on observational data, whereas rank *B* indicates less reliability owing to diminished observational influence on the variable and a greater dependence on the model.

Rank *C* indicates a variable that is fully model dependent, ie, direct observational data associated with the variable are unavailable (Kalnay *et al.*, 1996). For the variables used in this study, NNR ranks geopotential height and SLP as *A*, SAT as *B* and SPR as *C*.

Gridded reanalysis allows a more comprehensive assessment of climate in remote regions than does individual station analysis and is generally preferred in climate studies of the Arctic (Bromwich *et al.*, 2002). Some high-latitude studies, however, have revealed inaccuracies in certain NNR variables. For example, topographic smoothing related to the low resolution of gridded NNR oversimplifies mountainous terrain, which leads to inaccuracies in the derived modelled temperatures (Bromwich *et al.*, 2002). In the QEI, the potential for this error is greatest in its eastern sector, where topographic complexity is greatest. Compounding this problem is the paucity and variable quality of observational climate data from this region, which cause inhomogeneities in the assimilation data, especially in the early part of the record (pre-1958) when only limited radiosonde coverage occurred (Serreze and Barry, 2005: 257). Furthermore, only two long-term weather stations exist in the mountainous eastern sector of the QEI (Alert and Eureka), both of which are located in coastal lowlands, thereby limiting their climatic representation of this area (Maxwell, 1981).

Additional inaccuracies are associated with NNR modelled precipitation in the Arctic. Over land areas, NNR tends to overestimate summer precipitation, an effect resulting from excessive (modelled) convective precipitation (Serreze and Hurst, 2000). For the period of interest in this study (1949–2002), however; summer precipitation rate over the QEI is very low and any overestimation inherent to this variable is believed to have little impact on subsequent analyses (discussed below). NNR generated spatial patterns of precipitation rate has also been shown to be too simplistic, especially in its inability to produce observed interannual variability in snow cover (Serreze and Maslanik, 1997; Cullather *et al.*, 2000). Serreze *et al.* (2003) report consistent NNR underestimation of precipitation variability in Arctic regions, and similar accounts of underestimated precipitation variability are also noted by Bromwich *et al.* (2002) in their work over Baffin Island. Nevertheless, they noted that the normalized, long-term record still captures the relative variability in SPR, which is also true over the QEI.

### ERSST data

Climate variability is strongly linked to variations in oceanic boundary conditions (Hansen and Bezdek, 1996). Thus, the influence of Sea Surface Temperatures (SSTs) on variations in atmospheric cir-

culation is considered for high latitude regions. The Extended Reconstructed Sea Surface Temperature (ERSST v.2) data set (Smith and Reynolds, 2004) was obtained from the National Oceanic and Atmospheric Administration's Cooperative Institute for Research in Environmental Sciences (NOAA-CIRES), Climate Diagnostic Center (CDC) (<http://www.cdc.noaa.gov/cdc/data.noaa.ersst.html>). The ERSST v.2 was developed using the SST data and enhanced statistical techniques provided by the International Comprehensive Ocean–Atmosphere Data Set (ICOADS). The ERSST v.2 has a 2° latitude by 2° longitude grid, and was designed to manage more effectively regions with weak-variance while improving high-latitude SST analyses by using sea-ice concentration data (Smith and Reynolds, 2004).

## Analysis and discussion

This section presents a three-part analysis and discussion of the spatial changes in perennial snow and ice extent and ELA  $\Delta h$  between the LIA and 1960 in the QEI, as reported in Wolken *et al.* (2008, this issue). The first section analyses NCEP/NCAR reanalysis and identifies extreme cold and warm decades, and specific modes of variability associated with climatological variables in the modern record (1949–2002). These cold and warm decades serve as possible analogues for those that might have occurred between the LIA and the early twentieth century in the QEI. In the second section, important atmosphere–ocean interactions related to the assumed modern analogues of LIA and the early twentieth-century climates (cold and warm decades) are further identified and discussed. The third section identifies important connections between the pattern of ELA  $\Delta h$  and the primary modes of variability of climatological variables found in the modern record, and provides a spatial reconstruction of post-LIA to 1960 temperature change in the QEI.

### Climate variability: 1949–2002

In the QEI, variability in net mass balance is dominated by climate conditions during the summer (ie, temperature and precipitation). This is largely because winter accumulation is low and relatively consistent, allowing interannual variability in ablation to predominantly control variations in the height of the equilibrium-line (Dowdeswell *et al.*, 1997). It is, therefore, assumed that the reduction of perennial snow/ice extent since the LIA has also been dominated by changes in summer climate; if so, this reduction provides a proxy record of summer climate change. Hence, the variability in

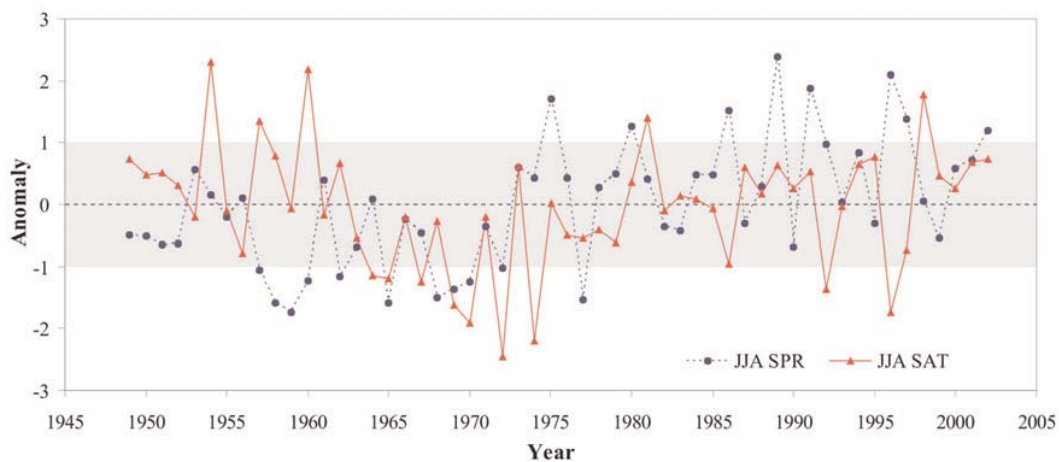


**Figure 2** Standardized anomaly time series of summer 2 m temperature (SAT; red) and winter surface precipitation rate (SPR; blue) for the period 1949–2002. Extreme years are those with standardized anomaly values exceeding one standard deviation

summer temperature and precipitation in the QEI between the end of the LIA and 1960 is of primary interest for this study. However, because the instrumental record in the QEI (~56 yr) extends only a decade into the record of ELA change (LIA to 1960), the contemporary record was searched for potential modern analogues of climatic conditions that would have favoured, and hence help to explain, the high summer ablation and the large spatial differences in  $\Delta h$  in the QEI during the early twentieth century (noted above).

All NNR variables were spatially averaged across the QEI based on a  $2.5^\circ$  resolution grid. All climate variables used in this study (NNR and ERSST) span the interval 1949–2002 and

annual, summer (JJA) and winter (SONDJFMAM) averages were obtained for each year. Long-term seasonal means (1949–2002) and standard deviations were calculated, and used to compute standardized anomalies from the long-term mean by,

$$X_N = (X_i - X_m)/S_x, \quad (1)$$

where  $X_i$  is the mean of a meteorological variable (annual or seasonal) for a particular year,  $X_m$  is the long-term mean (annual or seasonal), and  $S_x$  is the long-term standard deviation (annual or seasonal) for a meteorological variable.

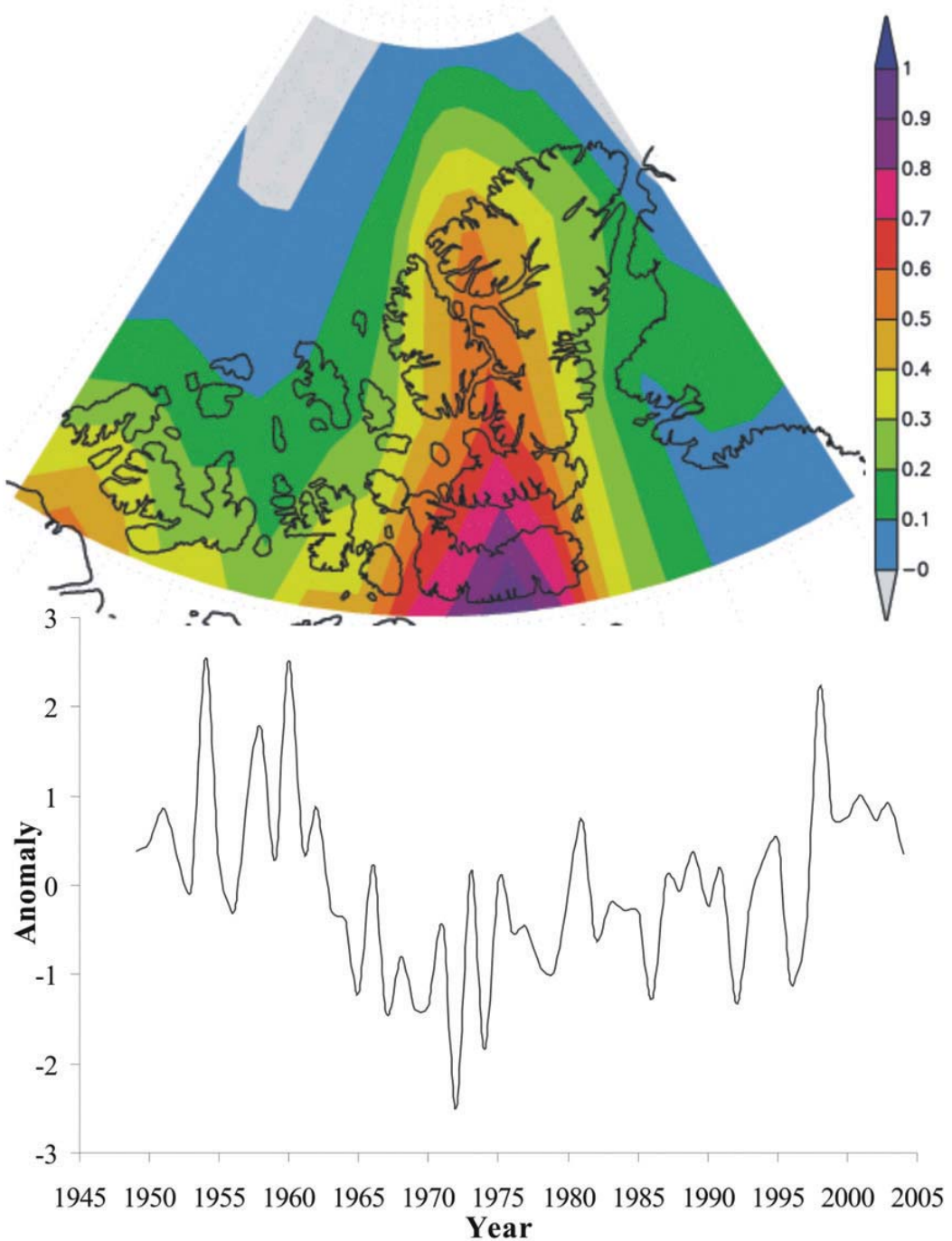


**Figure 3** The first Empirical Orthogonal Function (EOF-1) of SAT (top), centred over the QEI, and corresponding principal component (PC-1) time series (bottom) for the period 1949–2002

The NNR time series (1949–2002) of QEI standardized mean summer SAT and SPR anomalies are shown in Figure 2. Both temperature and precipitation records show substantial interannual variability, and only a slight correlation ( $r = 0.01$ ) is found between the two variables. Summer SAT anomalies in the time series range from  $-2.5$  to  $2.3$  standard deviations, equivalent to  $-1.0$  to  $0.9^{\circ}\text{C}$ . The highest (warmest) anomalies in the period occurred during the late 1950s to early 1960s, before a step-like change to the lowest (coldest) anomalies from the mid-1960s to mid-1970s. The period from the late 1970s to the present is characterized by less interannual variability with more positive temperature anomalies resulting in a gradual increase in mean summer

temperature. The time series contains nine extreme cold years (those exceeding one standard deviation: 1964, 1965, 1967, 1969, 1970, 1972, 1974, 1992 and 1996) and five extreme warm years (1954, 1957, 1960, 1981 and 1998). Seven of the cold years occurred during the mid-1960s to mid-1970s, with the coldest mean summer temperature (1972) falling  $0.9^{\circ}\text{C}$  below the 1949–2002 mean ( $-0.8^{\circ}\text{C}$ ). Three of the five warm years occurred during the warmer than normal part of the record, from the late 1950s to early 1960s; the warmest mean summer SAT for the entire record ( $0.1^{\circ}\text{C}$ ; 1954) reached  $0.9^{\circ}\text{C}$  above the 1949–2002 mean. QEI averaged winter SPR anomalies in the time series (1949–2002) range from  $-1.7$  to  $2.4$  standard deviations, and

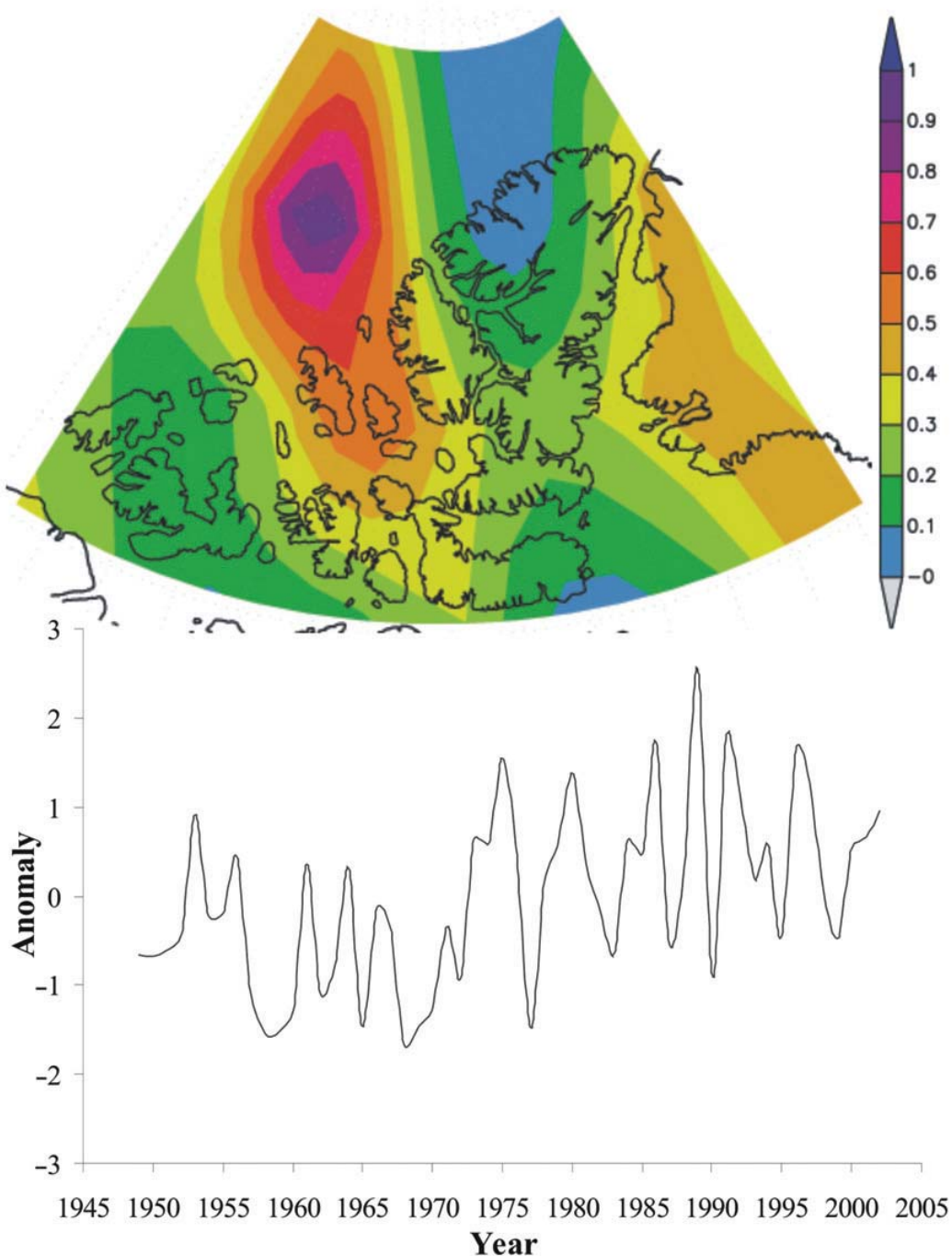


**Figure 4** EOF-1 of SPR (top), centred over the QEI, and corresponding PC-1 time series (bottom) for the period 1949–2002

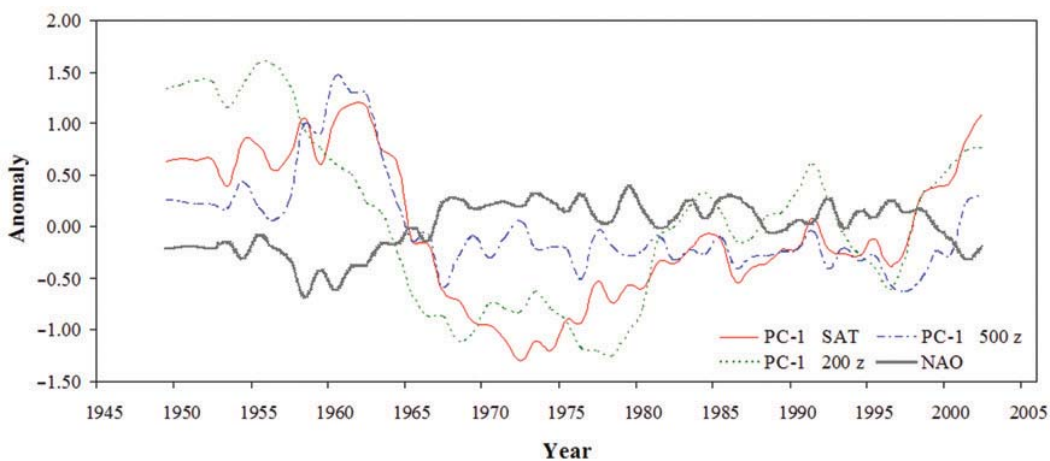


**Figure 5** Five-year running mean time series of the first principal components of SAT and 500 and 200 hPa geopotential heights, and standardized anomalies of the NAO index (1949–2002). In the early part of the record, strong decadal extremes are evident as each of the time series covary. During the latter part of the record decadal trend are much weaker, and interannual variability dominates

trends in the time series show drier than normal conditions in the first half of the record (1949–1974), with several extreme dry (1957–1960, 1962, 1965, 1968–1970 and 1972) but no extreme wet summers. The latter half of the record (1975–2002), however, shows wetter than normal conditions, with several extreme wet (1975, 1980, 1986, 1989, 1991–1992, 1996–1997 and 2002) and only one extreme dry summer (1977).

#### Patterns of variability

Empirical Orthogonal Functions (EOFs) provide a compressed description of the variability of a spatially distributed time series, often referred to as a mode of variability. Principal Components (PCs) associated with these modes of variability demonstrate how the EOFs oscillate in time. In this study, EOFs were used to describe the main modes of variability of NNR meteorological variables over the QEI for the 1949–2002 (summer) period. EOFs were computed to a cumulative explained variance of 80% for the following meteorological variables: SAT, SPR, SST, SLP and geopotential heights at 850, 500 and 200 hPa levels.

Figure 3 shows the leading mode of variability (EOF-1) for summer SAT for the QEI and the corresponding PC time series from 1949–2002. EOF-1 explains 55% of the variance (EOFs 2 and 3 explain 12 and 8%, respectively) and illustrates a strong pattern of variability over the eastern QEI. Higher values of variance occur in the southeast part of the islands (principally Devon Island) and extend northward into the intermontane basin between Axel Heiberg and Ellesmere Islands. The pattern of variability illustrated by EOF-1 (Figure 3) coincides with the pattern of ELA  $\Delta h$  (Wolken *et al.*, 2008, this issue: figure 11). The principal component time series associated with EOF-1 shows how this preferred temperature pattern evolves over time (Figure 3). The positive phase of this pattern was strongly established during the early part of the record, concomitant with the highest summer temperatures during the period (1949–2002). Conversely, negative scores (PC-1) of this mode are dominant from the mid 1960s to the late 1970s, indicating cool summer temperatures in the same spatial pattern.

EOF-1 of SPR (1949–2002) explains 40% of the variability in the period (Figure 4). The spatial pattern of variability shows a band of positive loadings extending from the north-central to east-central QEI, with the high values over the Arctic Ocean and running through Meighen Island and Amund and Ellef Ringnes

Islands. The associated PC time series (Figure 4) shows high interannual variability, with the first half of the record showing mainly negative anomalies in the SPR (1949–1974), whereas positive anomalies are prevalent during the latter part of the record (1975–2002). EOFs 2 and 3 (not shown) explain another 16 and 11% of the variability within the period of record, respectively.

The distinct pattern of variability that is expressed in EOF-1 of SPR represents the dominant storm track through the QEI. The QEI is situated between relatively high SLP associated with the perennially ice-covered Arctic Ocean and low SLP in the commonly open waters of Baffin Bay (Alt, 1987). This configuration causes cyclones to take a S-SE track through the QEI towards Baffin Bay, where there is an increase in cyclone frequency and cyclogenesis (Serreze and Barry, 2005: 98). Higher than normal precipitation occurs in the QEI when there is an increase in the frequency of cyclones along this track (ie, the positive phase of the leading EOF of SPR); however, anomalously low SPR during approximately the first half of the record (1949–1974) suggests a decrease in the frequency of cyclones following this S-SE trajectory through the QEI.

#### Correlations and decadal trends

Variations in summer temperature and precipitation in the QEI (1949–2002) are due in part to fluctuations in the distribution of atmospheric mass in the Arctic. PC-1 of QEI averaged summer SAT is positively correlated with summer geopotential height at the 500z and 200z levels ( $r = 0.57$  and  $0.59$ , respectively) and negatively correlated with the summer North Atlantic Oscillation (NAO) index ( $r = -0.48$ ). Only slight correlations, however, are apparent with other climate indices (eg, Pacific North American pattern (PNA),  $r = 0.19$ ; Southern Oscillation Index (SOI),  $r = 0.17$ ; Arctic Oscillation (AO),  $r = 0.03$ ). PC-1 of summer QEI SPR is negatively correlated with fluctuations in the height of the summer 500 hPa geopotential surface ( $r = -0.64$ ) and positively correlated with the summer AO index ( $r = 0.53$ ).

Figure 5 shows five-year running mean time series of the first principal components of QEI averaged summer SAT and summer geopotential height at the 500z and 200z levels, and the summer NAO index for the period 1949–2002. Decadal- and multidecadal-scale fluctuations in PC-1 of summer SAT are strongly coupled to changes in both the upper troposphere (500z) and lower stratosphere (200z). Moreover, decadal shifts in the phase of the NAO

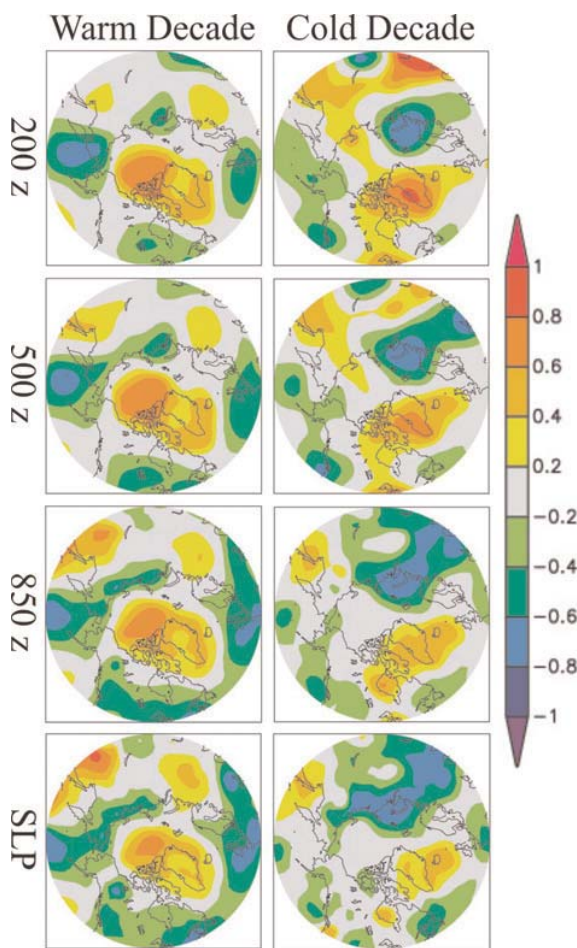


**Figure 6** Correlation coefficients for linear regression of PC-1 of QEI averaged SAT with SLP and 850, 500 and 200 hPa geopotential height surfaces (1949–2002) at each grid point north of 45°N

are coincident with decadal-scale modifications in PC-1 of summer SAT, which suggests regional-scale influences on summer surface temperature fluctuations in the QEI. Distinct trends in the time series in approximately the first half of the record illustrate contrasting periods of warm and cold conditions, which will serve as the basis for the following analyses.

### Warm and cold decades

Two decadal episodes representing extreme (exceeding one standard deviation of the decadal mean for the period 1949–2002) warm (1953–1962) and cold (1965–1974) periods are recoded in the NNR spatially averaged time series for the QEI. The warm decade is consistent with reports of net ablation on glaciers on the Hazen Plateau, E Ellesmere Island (Hattersley-Smith and Serson, 1973), and the cold decade is characterized by a lowering of the ELA and positive mass balance on some QEI glaciers and ice caps (Bradley and Miller, 1972; Bradley, 1973, 1975; Bradley and England, 1978a, b; Alt, 1987; Braun *et al.*, 2004). These contrasting temperature regimes are examined and analysed in order to identify potential modern analogues for LIA and early twentieth-century climates.

### Relation to atmospheric circulation

In order to examine the influence of atmospheric circulation patterns on summer SAT in the QEI during both warm and cold decades, PC-1 of QEI averaged summer SAT was regressed upon mean summer sea-level pressure and 850, 500 and 200 hPa geo-

tential height fields at each grid point north of 45°N (Figure 6). For the warm decade, anomalously high temperatures in the QEI are positively correlated with higher than normal SLP (Figure 7) and elevated geopotential heights up to 200z over the Canadian Arctic, most of the Arctic Basin and southeastwardly over Iceland, the western North Atlantic Ocean and the Labrador Sea (ie, a warm core high). In this region, a barotropic structure exists, that is, the positive geopotential anomaly occurs from the surface to the lower stratosphere, which coincides with a weak summer polar vortex, the centre of which lies northwest of the QEI over the Arctic Ocean (Figure 8). This barotropic structure is similar to that associated with the negative phase of the AO (Thompson and Wallace, 1998), and to a lesser extent with the NAO. Hence, a negative correlation exists between warm decade PC-1 of QEI averaged summer SAT and both the AO and NAO indices ( $r = -0.38$  and  $-0.57$ , respectively). During the cold decade, PC-1 of QEI averaged summer SAT is positively correlated with geopotential height at the 200 and 500 hPa levels over the QEI (Figure 6). In the lower troposphere, however, only a slight negative correlation exists between geopotential height (850 hPa to surface) and PC-1 (summer SAT) in the Arctic Basin and the western QEI, whereas, in the eastern Canadian Arctic, Greenland and Iceland a positive correlation occurs between these variables. In the Arctic basin and western QEI, a core of cold dense air resides in the lower troposphere, resulting in high SLP and anomalously high geopotential heights below ~850 hPa (ie, a cold core high; Figure 7). Above this surface high, a strong, QEI-proximal summer polar vortex occurs in the upper troposphere and lower stratosphere (Figure 8). From northern Ellesmere Island to southern Hudson Bay and eastwards across the North Atlantic, the negative geopotential anomaly occurs consistently from the lower troposphere to the lower stratosphere, while in the mid-Atlantic, areas of negative correlation represent positive geopotential anomaly (Figure 6). Anomalously low pressure in the North Atlantic relative to high pressure in the mid-Atlantic during the cold decade, is characteristic of a positive NAO (Figures 5 and 7); a negative correlation exists between PC-1 of QEI averaged summer SAT and the NAO index, but the correlation is weak ( $r = -0.32$ ).

### Atmosphere-ocean interactions

At high latitudes, complex energy exchanges between the atmosphere and ocean can occasion positive feedbacks affecting atmospheric circulation, SSTs, and SATs (Hansen and Bezdek, 1996; Mysak *et al.*, 1996; Rogers *et al.*, 1998). To investigate the influence of SST on temperature changes during the warm and cold decades across the QEI, PC-1 of mean summer SAT was regressed upon mean summer SST (using the ERSST reanalysis) at each grid point for the extended circumpolar region north of 45°N (Figure 9). During the warm decade, PC-1 of QEI averaged SAT is positively correlated with SST in the central and western North Atlantic, Labrador Sea and Hudson Bay and north into Baffin Bay and along the east coast of Greenland. In these areas, the correlation is robust ( $r = 0.65$ ) and the variation in summer SST explains approximately 42% of the variability in the mean summer temperature for the QEI. Additional areas of positive correlation also occur in the Bering Sea, extending northward through Bering Strait, as well as in the Gulf of Alaska. During the cold decade, PC-1 of QEI averaged SAT is positively correlated with SST across the North Atlantic, with the most robust correlation located in the east-central North Atlantic ( $r = 0.70$ ), where variation in summer SST accounts for about 50% of the variation in summer temperature in the QEI. Other areas of positive correlation are shown in Hudson Bay and the Labrador Sea, extending north into Davis Strait. Anomalously cool SAT in the QEI during this decade is negatively correlated with a broad area of warm SST in the North Pacific, as well as a much smaller area along the northeast coast of Greenland.

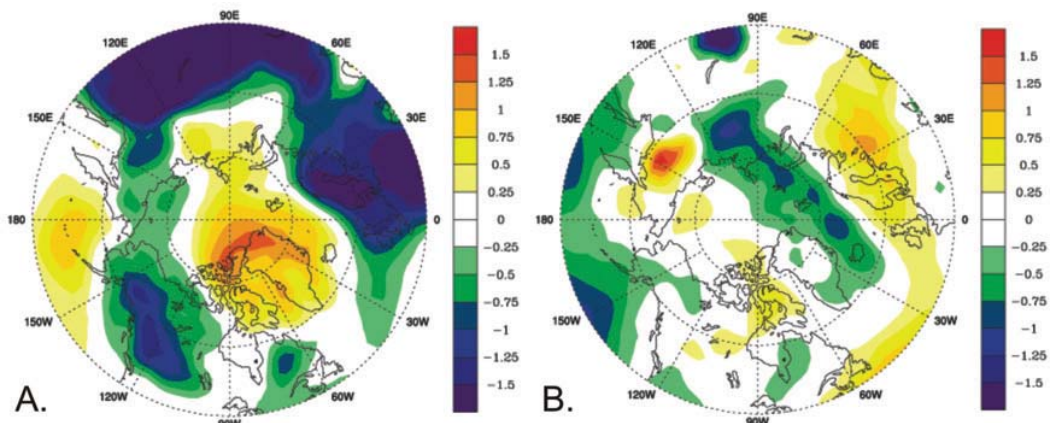


**Figure 7** Summer mean SLP anomalies ( $45\text{--}90^\circ\text{N}$ ) during warm (1953–1962) and cold (1965–1974) decades in the QEI. Anomalies are in reference to the 1949–2002 climatology period

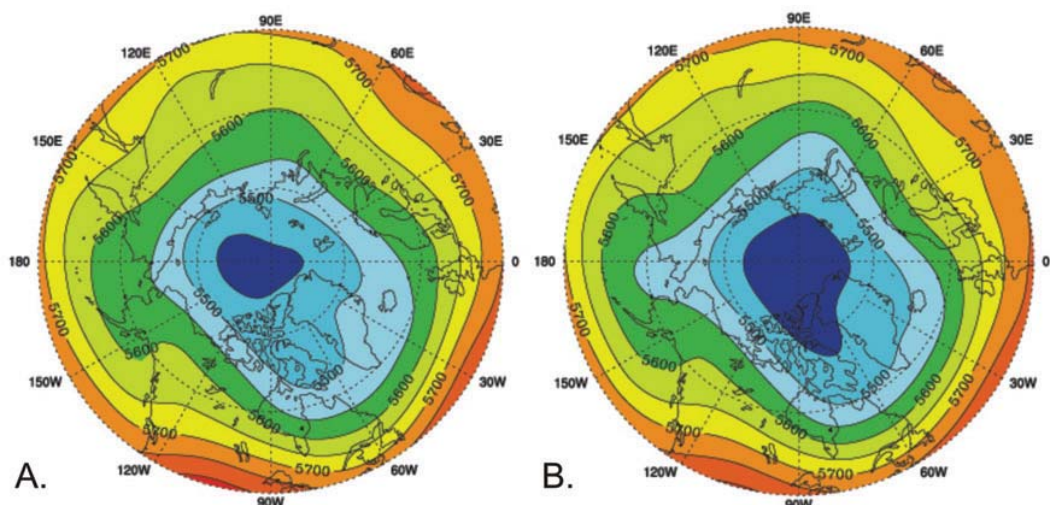


**Figure 8** Mean 500 hPa geopotential height surface indicating a weak, QEI-distal (strong, QEI-proximal) polar vortex during the warm (cold) decade

EOFs of summer SST were computed for the area north of  $45^\circ\text{N}$  for the period 1949–2002. Figure 10 shows the leading two EOFs and their corresponding principal component time series. EOF-1 accounts for 29% of the variance and depicts a spatial pattern of variability whereby positive loadings are in the North Pacific and Bering Strait and lesser positive values are in the North Atlantic. For the full period of record, a positive correlation is revealed between PC-1 of SST and PC-1 of QEI summer SAT ( $r = 0.32$ ), with a positive correlation during the warm decade ( $r = 0.32$ ) and a weak negative correlation during the cold decade ( $r = -0.10$ ). EOF-2 explains 18% of the variance in the data set and shows strongly positive values of variance in the North Atlantic, Davis Strait and Hudson Bay, and slightly negative values in the Bering Sea, Bering Strait and the Gulf of Alaska. A positive correlation was found between PC-2 of SST and PC-1 of QEI summer SAT for the period 1949–2002 ( $r = 0.54$ ), with stronger positive correlations during both the warm and cold decades ( $r = 0.65$  and  $0.76$ , respectively), explaining 42% (warm) and 58% (cold) of the variance in PC-1 of QEI SAT. Strong coupling in these time series reflects the influence of changes in SSTs in the North Atlantic on SAT in the QEI during both extreme decades (Figure 11).

The distribution of SST is largely influenced by surface winds resulting from strong gradients in the sea-level pressure fields. During the cold decade, anomalously low SSTs across the North Atlantic were influenced by enhanced westerly winds across the North Atlantic, resulting from lower than normal pressure near Iceland (extending northeast into the Greenland and Barents seas) in combination with anomalously high pressure in the central Atlantic. Although less intense, the cold decade atmospheric circulation pattern is similar to that of the 1972 extreme cold year described by Bromwich *et al.* (2002), where strong westerly winds across the North Atlantic increased the stress on the Ekman layer causing enhanced divergence and upwelling (lower SSTs) in the North Atlantic (Figure 9). In both patterns (cold decade and 1972), a deeper than normal Icelandic low was coupled with anomalously high pressure over the Arctic Ocean and the Canadian Arctic Archipelago, which created an intense zonal pressure gradient across the central and eastern QEI and Greenland and caused strong northerly airflow over this region. This persistent high pressure also serves as an effective obstruction to cyclones that typically track through this region (Alt, 1987), thereby reducing the precipitation during such cold intervals. Low SSTs in the North

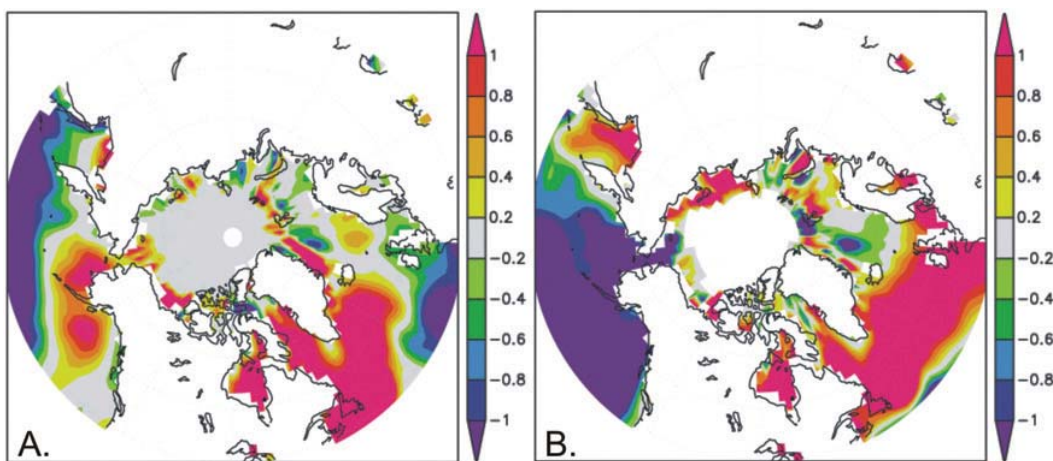


**Figure 9** Correlation coefficients of linear regression of PC-1 of QEI averaged SAT with SST (1949–2002) at each grid point north of 45°N

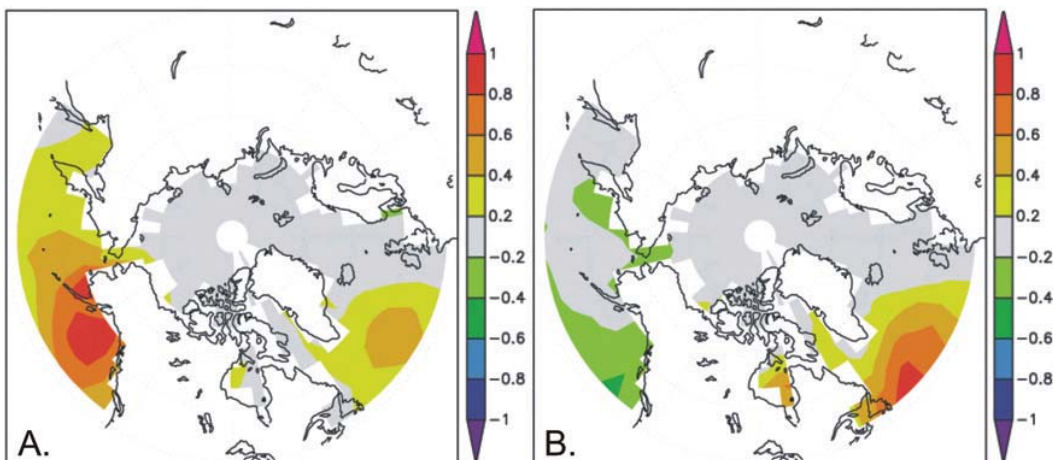


**Figure 10** First and second EOFs of summer SST (1949–2002) north of 45°N for the period 1949–2002

Atlantic increase low-level mid-latitude baroclinicity, resulting in enhanced low pressure over Iceland and stronger than normal cold northerly flow over the eastern Canadian Arctic (Bromwich *et al.*, 2002). In 1972, this northerly flow resulted in exceptionally low snowlines and positive summer mass balances on QEI glaciers (Alt, 1987), as well as one of the lowest percentages of summer open water on record throughout the QEI (Koerner, 1977). It has been hypothesized that the anomalous SSTs during the summer of 1972 were related to transient pools of cold water associated with the Great Salinity Anomaly (1968–1982; Dickson *et al.*, 1988; Rogers *et al.*, 1998; Bromwich *et al.*, 2002); it is possible that the migration of the salinity anomaly through the North Atlantic may have had an influence on the anomalous SSTs that were recorded during the cold decade, and ultimately, the low SATs throughout the QEI during this time. However, anomalously low SSTs in the North Pacific may also have influenced QEI SATs during the cold decade by modifying the Northern Hemisphere atmospheric circulation, which has also been credited for the abrupt lowering of summer freezing level heights over the QEI in 1963 (Bradley, 1973). Changes in the freezing level height in the atmosphere have been shown to be directly related to fluctuations in the ELA in the High Arctic (Bradley, 1975). Another influence on the low SAT across the QEI during the cold decade may have been the injection of volcanic aerosols into the stratosphere in response to increased volcanic activity during the 1960s and 1970s, starting with the

massive eruption of Mt Agung (Indonesia, 1963) (Bradley and England, 1978a, b; Hansen *et al.*, 1978).

During the warm decade, high SSTs in the W North Atlantic Ocean and the Labrador Sea coincided with lower than normal pressure over northern Quebec, and anomalously high pressure over Greenland and most of the Canadian Arctic Archipelago. The anomalous circulation pattern resulted in the cessation of typically strong westerly winds in the W North Atlantic, which, to first order, would have decreased the evaporative heat loss from the ocean surface layer. In addition, a pressure gradient reversal led to anomalous easterly wind stresses on the Ekman layer in this region, which would have caused a convergence of flow, leading to downwelling and a thickening of the warm surface layer in the western North Atlantic and Labrador Sea. Advection of warm water into Davis Strait and Baffin Bay would have significantly reduced sea-ice extent and increased the thermodynamic efficiency of warm southeasterly winds directed into the QEI, effectively increasing the ELA and enhancing ablation on perennial snow/ice masses in this region.

Temperature variability in the Arctic has also been linked to fluctuations in sea-ice extent (Chapman and Walsh, 1993; Parkinson *et al.*, 1999; Bengtsson *et al.*, 2004; Johannessen *et al.*, 2004). In order to examine the role of sea-ice extent in variations in QEI SAT during the extreme warm and cold decades, the 100 yr ‘Zakharov’ data set is used. This includes observations of Arctic

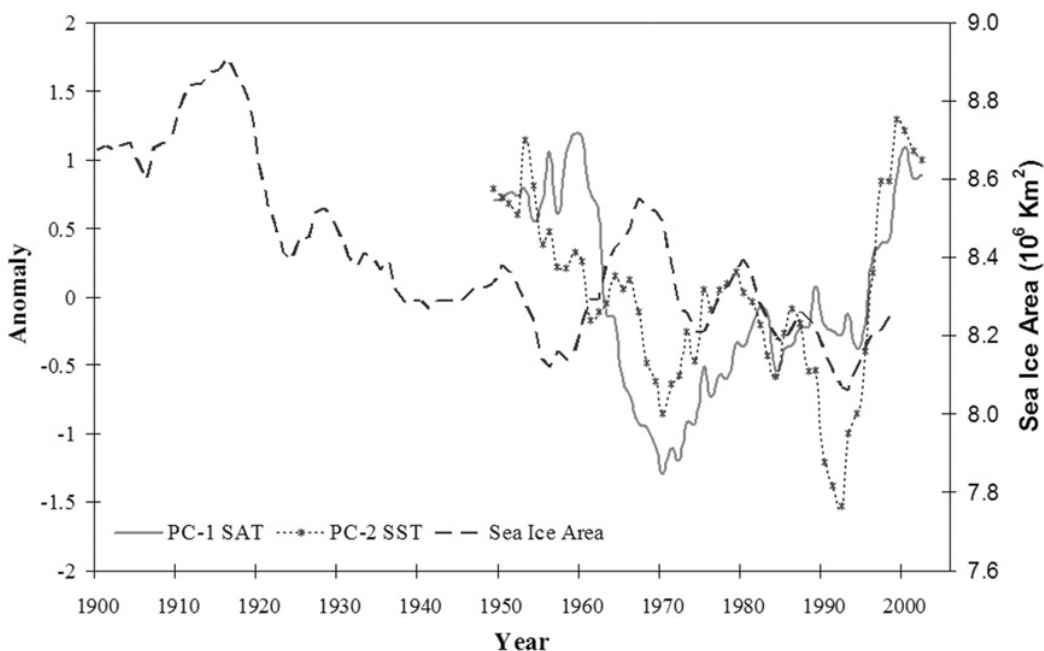


**Figure 11** Five-year running mean time series of sea-ice area (1900–1999) (Zakharov, 1997; Johannessen *et al.*, 2004), PC-1 of QEI averaged SAT (1949–1999), and PC-2 of summer SST (1949–2002) north of 45°N showing strongly coupled decadal and multidecadal variation during warm (1953–1962) and cold (1965–1974) decades in the QEI

sea-ice extent within the ice-ocean margin (Zakharov, 1997; Johannessen *et al.*, 2004). Figure 11 shows 5-yr running mean time series of PC-1 of summer SAT for the QEI compared with PC-2 of summer SST north of 45°N and mean annual sea-ice extent (1900 to 1999). SAT and sea-ice extent time series are negatively correlated ( $r = -0.31$ ) for the overlapping period of record (1949–1999), with stronger negative correlations occurring during both warm and cold decades ( $r = -0.52$ ). Thus, on decadal and multidecadal timescales, it is evident that QEI SAT co-varies with North Atlantic SST and Northern Hemisphere sea-ice extent. During the cold decade (1965–1974), the QEI experienced anomalously low mean summer temperatures ( $\sim -0.42^\circ\text{C}$  cooler), corresponding to the largest increase in sea-ice extent in the Arctic since the end of the LIA. In contrast, however, a pronounced decrease in sea-ice extent corresponds to the warm decade, when the mean summer SAT throughout the QEI was  $\sim 0.24^\circ\text{C}$  warmer than the 1949–2002 mean. These trends are also apparent in the early twentieth century, when anomalously low Arctic mean annual SATs ( $\sim 1900$ –1919) correspond to the largest sea-ice area during the century-long record, and anomalously high SATs ( $\sim 1920$ –1939) match a significant decrease in sea-ice extent (Figure 5, Johannessen *et al.*, 2004). This sizeable decrease in sea-ice extent is coincident with an increase ( $\sim 0.5$ – $1.0^\circ\text{C}$ ) in the observed spring/summer/autumn SAT across the QEI, likely marking the end of the LIA there (Figure 2, Johannessen *et al.*, 2004).

### ELA changes and twentieth-century analogues

The above analyses of climatic conditions in the QEI during the extreme cold and warm decades of the modern record, lead to the hypothesis that these decades can be used as analogues for describing climatic conditions that could be linked to LIA cooling and early twentieth-century warming in the QEI. Regional spatial variations in twentieth-century climate across the QEI are reflected in the change in the distribution of perennial snow/ice cover and ELA  $\Delta h$  between the end of the LIA and 1960 (Wolken *et al.*, 2008, this issue). Although the spatial distribution of  $\Delta h$

shows substantial meso- and microscale variability across the QEI, especially in the mountainous regions (where orographic effects are amplified), the data set also exhibits distinctive synoptic-scale patterns, indicative of regional climate forcing. For example, the area of greatest change in the ELA (Figure 11, Wolken *et al.*, 2008, this issue) is qualitatively similar to the pattern of the primary mode of summer temperature variability in the QEI (EOF-1, 1949–2002, Figure 3). This pattern shows the greatest amount of variability occurring in the eastern QEI, extending from central Devon Island northward across SW Ellesmere Island through the axis of Eureka Sound. The positive phase of EOF-1 (PC-1, summer SAT, Figure 3) characterizes the warm decade (1953–1962), when the mean temperature rose 1.5 standard deviations over the 1949–2002 mean (Figure 2). Strong qualitative similarities between EOF-1 (summer SAT) during the warm decade and the pattern of ELA  $\Delta h$  indicate that the warm decade may serve as a suitable analogue for climatic conditions during the early twentieth century that caused an increase in melt of perennial snow/ice masses across the QEI. Furthermore, dry conditions dominated throughout the QEI during the warm decade (Figures 2 and 4), and palaeoprecipitation proxy records from the central QEI suggest that similar dry conditions persisted there during the early twentieth century (Lamoureux, 2000). While the effect of low summer precipitation on net mass balance in the QEI is important (Dowdeswell *et al.*, 1997), such dry conditions indicate that the regional pattern of ELA  $\Delta h$  is largely a reflection of the variation in summer temperature.

Reconstructed temperature change across the QEI from the end of the LIA to 1960 is shown in Figure 12. This reconstruction is calculated from ELA  $\Delta h$  based on a summer near-surface temperature lapse rate of  $-4.3^\circ\text{C}/\text{km}$ , empirically derived from an observational network on Prince of Wales Icefield, Ellesmere Island (Figure 1; Marshall *et al.*, 2007). Resulting mean temperature change for the QEI was  $+1.1^\circ\text{C}$  ( $SD = 0.4^\circ\text{C}$ ), ranging from  $<0.5^\circ\text{C}$  along NW Axel Heiberg and Ellesmere Islands and W Melville Island, to  $>2.9^\circ\text{C}$  in localized areas of Ellesmere and Devon

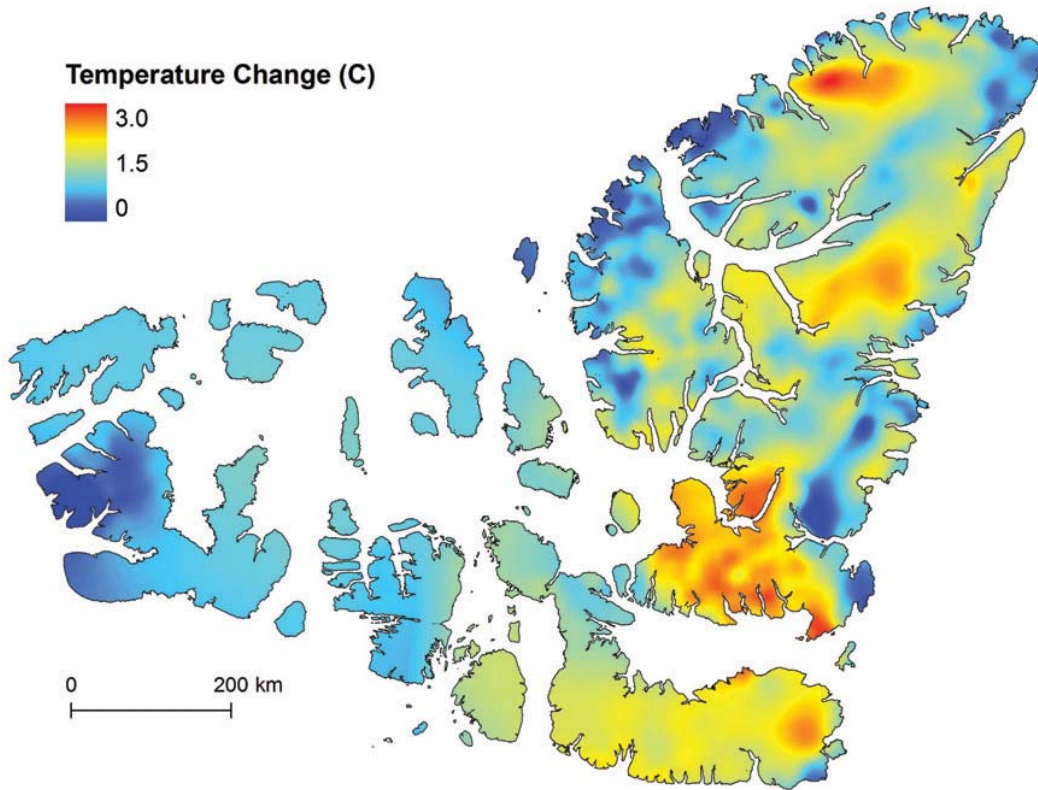


**Figure 12** Temperature change between the LIA and 1960, estimated from ELA  $\Delta h$  (Wolken et al., 2008, this issue) using a summer near-surface temperature lapse rate of  $-4.3^{\circ}\text{C}/\text{km}$  (Marshall et al., 2006)

Islands. The ELA-derived temperature changes are consistent with changes related to circum-Arctic gridded surface air temperatures (MJASO) during the early twentieth century (Figure 2, Johannessen et al., 2004), and they are also in broad agreement with other temperature reconstructions from the High Arctic. For instance, based on proxy data from lakes, ice cores, wetlands and marine sources Overpeck *et al.* (1997: figure 3) reported an average summer-weighted Arctic warming of  $\sim 1.5^{\circ}\text{C}$  from the end of the LIA to  $\sim 1960$ , with changes in the Canadian Arctic between 1 and  $3^{\circ}\text{C}$ . Also in the Canadian High Arctic, melt layer and  $\delta^{18}\text{O}$  analyses from ice cores extracted from the Devon and Agassiz ice caps (Figure 1) reveal marked warming in summer temperatures ( $\sim 0.5$  to  $1.5^{\circ}\text{C}$ ) between the end of the LIA and modern times (Koerner, 1977; Koerner and Fisher, 1990), which is broadly consistent with warming between the mid-nineteenth and the mid-twentieth centuries, as indicated by high sedimentation rates seen in lake core records from the QEI (Lamoureux and Bradley, 1996; Gajewski *et al.*, 1997; Lamoureux and Gilbert, 2004; Smith *et al.*, 2004) and by a rapid colonization of diatoms in QEI lakes in response to a reduction in lake-ice cover (Perren *et al.*, 2003).

Large-scale atmospheric circulation patterns during the cold and warm decades can also be used as analogues for those patterns that may have occurred during the LIA and the early twentieth century. Atmospheric circulation causing strong northerly flow into Arctic Canada during the cold decade is responsible for producing temperature anomalies in the QEI similar to those estimated from temperature reconstructions noted above. This atmospheric circulation pattern is similar to the synoptic types producing ‘cool and dry’ conditions (types 1, 4, 6 and 9) described by Bradley and England (1979), as well as the synoptic type I suggested by Alt (1987), which produces strong northerly flow through the QEI and is associated with melt suppression on QEI

ice caps. Although the seasonal atmospheric circulation patterns characterizing the cold decade produced temperatures comparable with those reported to have occurred during the LIA, other patterns observed in the contemporary record are capable of producing similar cool episodes, some of which are accompanied by increased precipitation (Bradley and England, 1979; Alt, 1987; Bromwich *et al.*, 2002). Indeed, some palaeoclimatic reconstructions for the central QEI suggest enhanced summer precipitation in these areas during the LIA (Lamoureux, 2000); some precipitation events during this time may have been related to increased volcanic activity (Lamoureux *et al.*, 2001).

One of the characteristic atmospheric circulation features during the warm decade in the Arctic is the strong S-SE flow across the QEI, which undoubtedly played a major role in the spatial distribution of positive SAT anomalies throughout this region. The similarity in the spatial pattern of temperatures reconstructed from ELA  $\Delta h$ , indicates that this circulation feature may also have been important during the post-LIA to 1960 period. However, other elements of high latitude atmospheric circulation have also been suggested to contribute to circum-Arctic warming during the early twentieth century. For instance, Bengtsson *et al.* (2004) propose that enhanced winter oceanic and atmospheric heat transport into the Arctic, initiated by an increase in the S-SW winds into the Barents Sea, was associated with regional warming that provided the main contribution to Arctic SAT anomalies from 1920 to 1940. While this feature does not appear during the winter months (NDJFMA) of the warm decade, there is indication of a possible pre-conditioning associated with the winter atmospheric circulation pattern (a weakened pressure gradient between the Icelandic low and central Atlantic high), which would have favoured warmer temperatures in the QEI during the warm decade summers.

## Conclusions

Reconstructed ELA trend surfaces modelled throughout the QEI represent important proxies of climate in a region with limited or no observational data during the late nineteenth and early twentieth centuries (Wolken *et al.*, 2008, this issue), and have been used here to assess climate variability and provide a model of the spatial variability of temperature and precipitation change in the QEI between the end of the LIA and 1960.

Warm (1953–1962) and cold (1965–1974) decades of summer SAT in the QEI were identified in the 1949–2002 NNR as potential analogs of LIA (cold) and early twentieth-century (warm) climates. The spatial pattern of  $\Delta h$  between the LIA and 1960 (Wolken *et al.*, 2008, this issue) is qualitatively similar to the primary mode of variability for mean summer SAT in the modern record (ie, EOF-1, 1949–2002, Figure 3), the positive (negative) phase of which is strongly in place during the warm (cold) decade. During the cold decade, lower than normal SATs are associated with atmospheric circulation patterns producing strong northerly winds over the study region. Warmer than normal SATs during the warm decade are linked to warm southeasterly flow through the QEI resulting from a pressure gradient reversal in the W North Atlantic, caused by anomalously high pressure over Greenland and the Canadian Arctic Archipelago coupled with lower than normal pressure over N Quebec and NW mainland Canada. SAT anomalies in the QEI during the warm (cold) decade are positively correlated with a weak (strong) QEI-distal (QEI-proximal) polar vortex, higher (lower) than normal SSTs in the North Atlantic, and lower (higher) Northern Hemisphere sea-ice extent.

Owing to the low precipitation in the QEI during both warm and cold decades, and its minimal influence on the pattern of ELA  $\Delta h$  compared with temperature,  $\Delta h$  is considered to reflect regional changes in summer SAT between the end of the LIA and 1960. Estimates of temperature change between the LIA and 1960 are calculated from  $\Delta h$  based on a summer near-surface temperature lapse rate of  $-4.3^{\circ}\text{C}/\text{km}$ . The mean estimated temperature change in the QEI from the LIA to 1960 is  $1.1^{\circ}\text{C}$ , and ranges from  $<0.5^{\circ}\text{C}$  near the northwest coasts of Axel Heiberg and Ellesmere Islands and the west coast of Melville Island, to  $>2.9^{\circ}\text{C}$  in the mountains of Ellesmere Island. While the large-scale atmospheric circulation changes required to produce this warming are not clear, plausible circulation patterns based on modern analogues have been proposed.

Investigating and understanding ice mass responses to past changes in climate is imperative to our understanding of future modifications to the cryosphere. Data presented in this study (and Wolken *et al.*, 2008, this issue) demonstrate the extent to which ice reduction occurred in the QEI in response to an average estimated temperature increase of  $1.1^{\circ}\text{C}$  between the end of the LIA and 1960, and highlight the sizable changes in sea ice extent during this same interval. These data are particularly important for providing a perspective on the continued warming and melt in the Arctic (Krabill *et al.*, 1999; Arendt *et al.*, 2002; Burgess and Sharp, 2004; Abdalati *et al.*, 2004) and the accelerated warming seen globally (Mann *et al.*, 1998). Furthermore, this study helps to clarify the considerable sensitivity of both terrestrial- and sea-ice systems to small changes in summer temperature, reinforcing the changes that will continue under ongoing global warming.

## Acknowledgements

This work was financially supported by the Natural Sciences and Engineering Research Council of Canada (NSERC Discovery Grant A6680) and the NSERC Northern Chair Award, both to J. England. Additional support to G. Wolken was provided by the Canadian Circumpolar Institute (University of Alberta, Edmonton, Alberta).

The Polar Continental Shelf Project, Natural Resources Canada, provided logistical support during the summers of 2001 and 2003 (PCSP/ÉPCP contribution # 003-07). Grants awarded to M. Sharp from the Meteorological Service of Canada CRYSYS (Cryospheric System to Monitor Global Change in Canada) programme and from the GLIMS (Global Land Ice Measurements from Space) project provided access to satellite data used in the study. We express our gratitude to R. Bradley (University of Massachusetts), A. Bush (University of Alberta) and D. Hik (University of Alberta) for their comments on an earlier draft of the manuscript. We also thank Atle Nesje and an anonymous referee for their comments and suggestions of how to improve this manuscript.

## References

- Abdalati, W., Krabill, W., Frederick, E., Manizade, S., Martin, C., Sonntag, J., Swift, R., Thomas, R., Yungel, J. and Koerner, R. 2004: Elevation changes of ice caps in the Canadian Arctic Archipelago. *Journal of Geophysical Research-Earth Surface* 109, doi:10.1029/2003JF000045.
- Alt, B.T. 1987: Developing synoptic analogs for extreme mass balance conditions on Queen Elizabeth Island ice caps. *Journal of Climate and Applied Meteorology* 26, 1605–23.
- Arctic Climate Impact Assessment 2004: *Arctic climate impacts assessment*. Cambridge University Press, 1046 pp.
- Arendt, A.A., Echelmeyer, K.A., Harrison, W.D., Lingle, C.S. and Valentine, V.B. 2002: Rapid wastage of Alaska glaciers and their contribution to rising sea level. *Science* 297, 382–86.
- Bengtsson, L., Semenov, V.A. and Johannessen, O.M. 2004: The early twentieth-century warming in the Arctic – a possible mechanism. *Journal of Climate* 17, 4045–57.
- Bradley, R.S. 1973: Recent freezing level changes and climatic deterioration in the Canadian Arctic archipelago. *Nature* 243, 398–400.
- 1975: Equilibrium-line altitudes, mass balance, and July freezing-level heights in the Canadian High Arctic. *Journal of Glaciology* 14, 267–74.
- Bradley, R.S. and England, J. 1978a: Volcanic dust influences on glacier mass balance at high latitudes. *Nature* 271, 736–38.
- 1978b: Recent climatic fluctuations of the Canadian High Arctic and their significance for glaciology. *Arctic and Alpine Research* 10, 715–31.
- 1979: Synoptic climatology of the Canadian High Arctic. *Geografiska Annaler* 61, 187–201.
- Bradley, R.S. and Miller, G.H. 1972: Recent climatic change and increased glaciation in Eastern Canadian Arctic. *Nature* 237, 385–87.
- Braun, C., Hardy, D.R. and Bradley, R.S. 2004: Mass balance and area changes of four High Arctic plateau ice caps, 1959–2002. *Geografiska Annaler Series A-Physical Geography* 86A, 43–52.
- Bromwich, D.H., Toracinta, E.R. and Wang, S.H. 2002: Meteorological perspective on the initiation of the Laurentide Ice Sheet. *Quaternary International* 95, 113–24.
- Burgess, D.O. and Sharp, M.J. 2004: Recent changes in areal extent of the Devon Ice Cap, Nunavut, Canada. *Arctic, Antarctic, and Alpine Research* 36, 261–71.
- Chapman, W.L. and Walsh, J.E. 1993: Recent variations of sea ice and air-temperature in high-latitudes. *Bulletin of the American Meteorological Society* 74, 33–47.
- Cullather, R.I., Bromwich, D.H. and Serreze, M.C. 2000: The atmospheric hydrologic cycle over the Arctic basin from reanalyses. Part I: comparison with observations and previous studies. *Journal of Climate* 13, 923–37.
- Dickson, R.R., Meincke, J., Malmberg, S.A. and Lee, A.J. 1988: The great salinity anomaly in the northern North-Atlantic 1968–1982. *Progress in Oceanography* 20, 103–51.
- Dowdeswell, J.A., Hagen, J.O., Bjornsson, H., Glazovsky, A.F., Harrison, W.D., Holmlund, P., Jania, J., Koerner, R.M., Lefauconnier, B., Omannay, C.S.L. and Thomas, R.H. 1997: The mass balance of circum-Arctic glaciers and recent climate change. *Quaternary Research* 48, 1–14.

- Dyurgerov, M.B. and Meier, M.F.** 1997: Mass balance of mountain and subpolar glaciers: a new global assessment for 1961–1990. *Arctic and Alpine Research* 29, 379–91.
- Edlund, S.A. and Alt, B.T.** 1989: Regional congruence of vegetation and summer climate patterns in the Queen Elizabeth Islands, Northwest Territories, Canada. *Arctic* 42, 3–23.
- Gajewski, K., Hamilton, P.B. and McNeely, R.** 1997: A high resolution proxy-climate record from an arctic lake with annually-laminated sediments on Devon Island, Nunavut, Canada. *Journal of Paleolimnology* 17, 215–25.
- Grove, J.M.** 2001: The initiation of the ‘Little Ice Age’ in regions round the North Atlantic. *Climatic Change* 48, 53–82.
- Hansen, D.V. and Bezdek, H.F.** 1996: On the nature of decadal anomalies in North Atlantic sea surface temperature. *Journal of Geophysical Research-Oceans* 101, 8749–58.
- Hansen, J.E., Wang, W.C. and Lacis, A.A.** 1978: Mount Agung eruption provides test of a global climatic perturbation. *Science* 199, 1065–68.
- Hattersley-Smith, G. and Serson, H.** 1973: Reconnaissance of a small ice cap near St. Patrick Bay, Robeson Channel, Northern Ellesmere Island, Canada. *Journal of Glaciology* 12, 417–21.
- Intergovernmental Panel on Climate Change (IPCC)** 2001: *Climate change 2001: the scientific basis*. Cambridge University Press, 408 pp.
- Johannessen, O.M., Shalina, E.V. and Miles, M.W.** 1999: Satellite evidence for an Arctic sea ice cover in transformation. *Science* 286, 1937–39.
- Johannessen, O.M., Bengtsson, L., Miles, M.W., Kuzmina, S.I., Semenov, V.A., Alekseev, G.V., Nagurnyi, A.P., Zakharov, V.F., Bobylev, L.P., Pettersson, L.H., Hasselmann, K. and Cattle, A.P.** 2004: Arctic climate change: observed and modelled temperature and sea-ice variability. *Tellus Series a-Dynamic Meteorology and Oceanography* 56, 328–41.
- Kalnay, E., Kanamitsu, M., Kistler, R., Collins, W., Deaven, D., Gandin, L., Iredell, M., Saha, S., White, G., Woollen, J., Zhu, Y., Chelliah, M., Ebisuzaki, W., Higgins, W., Janowiak, J., Mo, K.C., Ropelewski, C., Wang, J., Leetmaa, A., Reynolds, R., Jenne, R. and Joseph, D.** 1996: The NCEP/NCAR 40-year reanalysis project. *Bulletin of the American Meteorological Society* 77, 437–71.
- Kistler, R., Kalnay, E., Collins, W., Saha, S., White, G., Woollen, J., Chelliah, M., Ebisuzaki, W., Kanamitsu, M., Kousky, V., van den Dool, H., Jenne, R. and Fiorino, M.** 2001: The NCEP-NCAR 50-year reanalysis: monthly means CD-ROM and documentation. *Bulletin of the American Meteorological Society* 82, 247–67.
- Koerner, R.M.** 1977: Ice thickness measurements and their implications with respect to past and present ice volumes in the Canadian High Arctic ice caps. *Canadian Journal of Earth Sciences* 14, 2697–705.
- Koerner, R.M. and Fisher, D.A.** 1990: A record of Holocene summer climate from a Canadian high-Arctic ice core. *Nature* 343, 630–31.
- Krabill, W., Frederick, E., Manizade, S., Martin, C., Sonntag, J., Swift, R., Thomas, R., Wright, W. and Yungel, J.** 1999: Rapid thinning of parts of the southern Greenland ice sheet. *Science* 283, 1522–24.
- Lamoureux, S.** 2000: Five centuries of interannual sediment yield and rainfall-induced erosion in the Canadian High Arctic recorded in lacustrine varves. *Water Resources Research* 36, 309–18.
- Lamoureux, S.F. and Bradley, R.S.** 1996: A late Holocene varved sediment record of environmental change from northern Ellesmere Island, Canada. *Journal of Paleolimnology* 16, 239–55.
- Lamoureux, S.F. and Gilbert, R.** 2004: A 750-yr record of autumn snowfall and temperature variability and winter storminess recorded in the varved sediments of Bear Lake, Devon Island, Arctic Canada. *Quaternary Research* 61, 134–47.
- Lamoureux, S.F., England, J.H., Sharp, M.J. and Bush, A.B.G.** 2001: A varve record of increased ‘Little Ice Age’ rainfall associated with volcanic activity, Arctic Archipelago, Canada. *The Holocene* 11, 243–49.
- Mann, M.E., Bradley, R.S. and Hughes, M.K.** 1998: Global-scale temperature patterns and climate forcing over the past six centuries. *Nature* 392, 779–87.
- Marshall, S.J., Sharp, M.J., Burgess, D.O. and Anslow, F.S.** 2007: Near-surface temperature lapse rates on the Prince of Wales Icefield, Ellesmere Island, Canada: implications for regional downscaling of temperature. *International Journal of Climatology* 27, 385–98.
- Maxwell, J.B.** 1981: Climatic regions of the Canadian Arctic islands. *Arctic* 34, 225–40.
- Mysak, L.A., Ingram, R.G., Wang, J. and van der Baaren, A.** 1996: The anomalous sea-ice extent in Hudson Bay, Baffin Bay and the Labrador Sea during three simultaneous NAO and ENSO episodes. *Atmosphere-Ocean* 34, 313–43.
- Overpeck, J.K., Hughen, K., Hardy, D., Bradley, R., Case, R., Douglas, M., Finney, B., Gajewski, K., Jacoby, G., Jennings, A., Lamoureux, S., Lasca, A., MacDonald, G., Moore, J., Retelle, M., Smith, S., Wolfe, A. and Zielinski, G.** 1997: Arctic environmental change of the last four centuries. *Science* 278, 1251–56.
- Parkinson, C.L., Cavalieri, D.J., Gloersen, P., Zwally, H.J. and Comiso, J.C.** 1999: Arctic sea ice extents, areas, and trends, 1978–1996. *Journal of Geophysical Research-Oceans* 104, 20837–56.
- Perren, B.B., Bradley, R.S. and Francus, P.** 2003: Rapid lacustrine response to recent High Arctic warming: a diatom record from Sawtooth Lake, Ellesmere Island, Nunavut. *Arctic Antarctic and Alpine Research* 35, 271–78.
- Rogers, J.C., Wang, C.C. and McHugh, M.J.** 1998: Persistent cold climatic episodes around Greenland and Baffin Island: links to decadal-scale sea surface temperature anomalies. *Geophysical Research Letters* 25, 3971–74.
- Serreze, M.C. and Barry, R.G.** 2005: *The Arctic climate system*. Cambridge University Press, 402 pp.
- Serreze, M.C. and Hurst, C.M.** 2000: Representation of mean Arctic precipitation from NCEP-NCAR and ERA reanalyses. *Journal of Climate* 13, 182–201.
- Serreze, M.C. and Maslanik, J.A.** 1997: Arctic precipitation as represented in the NCEP/NCAR reanalysis. *Annals of Glaciology* 25, 429–33.
- Serreze, M.C., Clark, M.P. and Bromwich, D.H.** 2003: Monitoring precipitation over the Arctic terrestrial drainage system: data requirements, shortcomings, and applications of atmospheric reanalysis. *Journal of Hydrometeorology* 4, 387–407.
- Smith, S.V., Bradley, R.S. and Abbott, M.B.** 2004: A 300 year record of environmental change from Lake Tuborg, Ellesmere Island, Nunavut, Canada. *Journal of Paleolimnology* 32, 137–48.
- Smith, T.M. and Reynolds, R.W.** 2004: Improved extended reconstruction of SST (1854–1997). *Journal of Climate* 17, 2466–77.
- Thompson, D.W.J. and Wallace, J.M.** 1998: The Arctic Oscillation signature in the wintertime geopotential height and temperature fields. *Geophysical Research Letters* 25, 1297–300.
- Vinnikov, K.Y., Robock, A., Stouffer, R.J., Walsh, J.E., Parkinson, C.L., Cavalieri, D.J., Mitchell, J.F.B., Garrett, D. and Zakharov, V.F.** 1999: Global warming and northern Hemisphere sea ice extent. *Science* 286, 1934–37.
- Wolken, G.J., England, J.H. and Dyke, A.S.** 2008: Changes in late-Neoglacial perennial snow/ice extent and equilibrium-line altitudes in the Queen Elizabeth Islands, Arctic Canada. *The Holocene* 18, 000–000, this issue.
- Zakharov, V.F.** 1997: *Sea ice in the climate system*. WMO Technical Document 782. World Climate Research Programme, Arctic Climate System Study, 80.